# Investigation of Tuning Characteristics of Electrically Tunable Long-Period Gratings With a Precise Four-Layer Model

Qin Chen, Jonathan Lee, Minren Lin, Yong Wang, Stuart (Shizhuo) Yin, *Senior Member, IEEE*, Qiming Zhang, *Senior Member, IEEE*, and Karl M. Reichard, *Member, IEEE*

***Abstract*—In this paper, an investigation of the tuning characteristics of electrically tunable long-period gratings (LPGs) is presented. A precise four-layer model is used to quantitatively analyze the tuning potential of the gratings, and experimental data are provided to support the analysis. The four-layer model includes a silica core layer with an inscribed LPG, a thin silica cladding layer ($\sim$ 40 $\mu$m), an ultrathin ($\sim$ 50 nm) high refractive index indium–tin dioxide (ITO) inner electrode layer, and a tunable electrooptic (E-O) polymer layer. It has been found that the inner electrode layer, made of high refractive index ITO, can be modeled as a high refractive index overlay and causes the forward-propagating modes in the thin silica cladding to reorganize as the ambient refractive index changes. This reorganization effect can lead to a significant increase (ten plus fold) in the tuning range of LPG tunable filters. Moreover, the required specifications of the tunable polymer layer are quantitatively analyzed. Finally, the required characteristics of the E-O polymer is realized by using a nanocomposite ferroelectric relaxor poly(vinylidene fluoride-trifluoroethylene-chlorofluoroethylene) terpolymer.**

***Index Terms*—Electrooptic devices, electrooptic polymers, high index overlay, long-period fiber gratings, nanocomposite, optical fiber devices, optical fiber filters.**

## I. Introduction

FIBER GRATINGS have been extensively used in many areas of fiber optics [1]. Recently, a great deal of efforts have been devoted to the fabrication and study of long-period fiber gratings (LPGs), which are promising candidates for gain equalizers, band-rejection filters, sensors, etc. [2]. An LPG is a grating whose period is usually between 100 and 1000 $\mu$m, which is much longer than the wavelength of light propagating in the fiber. The function of a fiber grating depends on the mode coupling induced by the grating. For LPGs, the core mode(s) is coupled to the forward-propagating cladding modes. Because cladding modes experience very large scattering and bending losses, they attenuate quickly as they propagate, resulting in a rejection band in the grating transmission. One attractive aspect of the LPG is that its resonant wavelength can be easily tuned, which makes it a good candidate for an all-fiber tunable filter. Several tuning mechanisms, including microfluidic tuning [3], thermal tuning [4], strain tuning [5], and electrooptic (E-O) tuning [6], [7], have been investigated.

Compared to other tuning mechanisms, E-O tuning has the advantages of no moving parts, high speed, compact size, easy fabrication, and good long-term reliability. To achieve a large tuning range, an E-O material with a large refractive index change is needed. Recently, we reported the observation of giant electromechanical and E-O responses in both high energy electron irradiated poly(vinylidene fluoride-trifluoroethylene) copolymer and poly(vinylidene fluoride-trifluoroethylene-chlorofluoroethylene) terpolymer [8]–[10]. Thus, this class of polymer is an excellent candidate for fabricating the LPG-based tunable filter.

More recently, it was found that the presence of a thin high refractive index overlay could induce strong changes in the distribution of the cladding modes, leading to a lowering of the mode bounding factor and consequently enhancing the evanescent wave interaction with the surrounding medium [11]–[13]. In our reported tunable filter design [6], [7], an ultrathin (tens of nanometers) indium–tin dioxide (ITO) layer is coated between the thin silica cladding layer and the E-O polymer layer to provide the required electric field across the E-O polymer. Because the refractive index of the ITO is higher than the silica, this ITO layer can serve not only as an electrode but also as an intrinsic high-index overlay, which in turn can significantly enhance the tuning range of the tunable filter.

To quantitatively investigate this tuning enhancement effect, a precise four-layer model, which includes the ITO overlay, is presented. The numerical results from the model are then compared to our experimental results. Both the theoretical analysis and the experimental results show that a significant increase in the tuning range (ten plus fold) can be achieved with the high-index ITO electrode layer.

## II. Theoretical Analysis

Fig. 1(a) and (b) illustrate the schematic structure of the E-O tunable LPG filter and the corresponding cross-sectional view, which includes six layers, namely 1) the silica core layer;

Manuscript received March 2, 2006; revised April 13, 2006. This work was supported by the National Science Foundation Materials Research Science and Engineering Center (NSF MRSEC) for Nanoscale Science under Grant DMR-0080019 and by the Naval Air Systems Command under Contract N00421-03-D-0044, Delivery Order Number 01.

Q. Chen, J. Lee, M. Lin, Y. Wang, S. Yin, and Q. Zhang are with the Department of Electrical Engineering, Pennsylvania State University, University Park, PA 16802 USA (e-mail: quc101@psu.edu; jel236@psu.edu; mxl18@psu.edu; yuw113@psu.edu; sxy105@psu.edu; qxz1@psu.edu).

K. M. Reichard is with the Applied Research Laboratory, Pennsylvania State University, University Park, PA 16802 USA (e-mail: kmr5@psu.edu).

Digital Object Identifier 10.1109/JLT.2006.876091

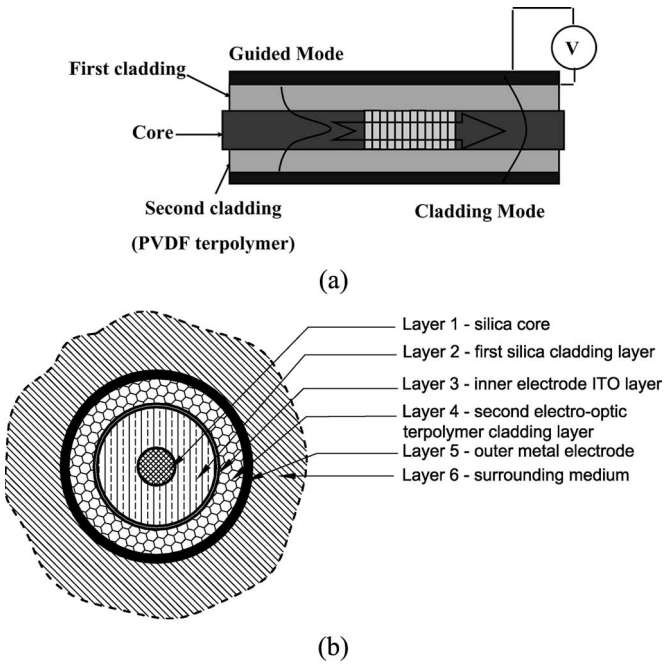


Fig. 1. (a) Schematic structure of the E-O tunable LPG filter. (b) Cross-sectional view of the E-O tunable LPG filter.

2) the thin silica cladding layer; 3) the inner ITO electrode layer; 4) the E-O polymer layer; 5) the outer metal electrode layer; and 6) the surrounding medium. The tuning characteristics of this filter may be quantitatively analyzed in the following way. As aforementioned, an LPG couples light from the propagating core mode to copropagating cladding modes. In a standard LPG, the phase matching between the core mode and the $i$th forward-propagating cladding mode is achieved at resonant wavelengths given by [11], [13]

$$\frac{2\pi}{\lambda}\left(n_{\text{eff}}^{\text{co}-1}-n_{\text{eff}}^{\text{cl}-i}\right)+s_o\left(\xi_{1,1}(\lambda)-\xi_{i,i}(\lambda)\right)=\frac{2\pi}{\Lambda} \tag{1}$$

where $n_{\text{eff}}^{\text{co}-1}$ is the effective refractive index of the core mode, $n_{\text{eff}}^{\text{cl}-i}$ is the effective refractive index of the $i$th radial order cladding mode in the thin silica cladding layer, $s_o$ is the coefficient of the first Fourier component of the grating, $\xi_{1,1}$ and $\xi_{i,i}$ are the self-coupling coefficients of the core and the $i$th cladding modes, respectively, and $\Lambda$ is the grating pitch. Because the effective refractive indices of the silica cladding modes are strongly dependent on the refractive index of the outside layers, the Bragg resonant wavelength of the filter, as given in (1), can be tuned by adjusting the refractive index of the outside layers. Although, theoretically speaking, $n_{\text{eff}}^{\text{cl}-i}$ depends on the refractive indices of all outside layers [i.e., layers 3–6, as shown in Fig. 1(b)], the influence from layers 5 and 6 can be negligible because they are far from the silica cladding layer. Thus, we can use a four-layer model (i.e., only considering layers 1–4) to analyze the tuning characteristics of the filter.

The general strategy used to theoretically calculate the LPG characteristics usually involves two steps. First, the propagation constants and mode profiles of the guided and cladding modes are calculated. Second, the coupling between the guided and cladding modes is found using coupling mode theory. In the last few years, several simulation approaches have been developed [14]–[16]. For example, Erdogan proposed a three-layer model in which the fields were solved precisely [14]. However, this three-layer model did not consider the ITO overlay layer and could not be used to precisely analyze our tunable filer. Another approach, developed by Anemogiannis *et al.* [15], used the transfer matrix method together with the LP approximation to solve for the eigenmodes. However, for our E-O tunable LPG filter, we need a model that can simulate structures with an arbitrary number of layers with an arbitrary refractive index profile while maintaining a relatively high calculation speed. Additionally, to achieve high precision in all different cases, it is preferable to avoid the use of LP approximation. Therefore, in this paper, we adopt a combination of the matrix method for eigenmode calculation introduced by Yeh and Lindgren [16] and the coupling mode formalism presented by Erdogan in the simulation.

In an optical fiber, the electric field of eigenmode along the propagating direction (longitudinal component) has a general form of $E_z(r,\theta,z,t)=E_z(r)e^{i\nu\theta}e^{i\beta z}e^{-i\omega t}$, where $r$, $\theta$, and $z$ are the radial, azimuthal, and axial components in cylindrical coordinates, respectively; $\nu$ is the azimuthal order of the mode; $\beta$ is the propagation constant of the mode; $\omega$ is the angular frequency of the propagating light; and $E_z(r)$ is the radial dependence of the electric field, which is governed by the Bessel equation

$$\frac{d^2E_z(r)}{dr^2}+\frac{1}{r}\frac{dE_z(r)}{dr}+\left[\left(k_m^2-\beta^2\right)-\frac{\nu^2}{r^2}\right]E_z(r)=0. \tag{2}$$

A similar relation holds for the magnetic field $H_z(r)$. Once the longitudinal components are found, the transverse components can be easily obtained through the relation between the longitudinal and transverse components [17].

If $n_{\text{eff}}>n_i$, where $n_{\text{eff}}$ is the effective refractive index of the mode and $n_i$ is the refractive index of the $i$th layer, a general solution of Bessel's equation in an $m+1$ layer structure has the form

$$\begin{aligned}E_z^{(i)}(r)&=C_iJ_\nu(p_ir)+C_i'Y_\nu(p_ir)\\H_z^{(i)}(r)&=jD_iJ_\nu(p_ir)+jD_i'Y_\nu(p_ir)\\p_i^2&=(k_in_i)^2-\beta^2\end{aligned} \tag{3}$$

where $J_v$ and $Y_v$ are the Bessel functions of the first and second kinds of order $v$, respectively, and $C_i$, $C_i'$, $D_i$, and $D_i'$ are the four constants for the $i$th layer. On the other hand, if $n_{\text{eff}}<n_i$, the general solution takes the form

$$\begin{aligned}E_z^{(i)}(r)&=C_iI_\nu(q_ir)+C_i'K_\nu(q_ir)\\H_z^{(i)}(r)&=jD_iI_\nu(q_ir)+jD_i'K_\nu(q_ir)\\q_i^2&=\beta^2-(k_in_i)^2\end{aligned} \tag{4}$$

where $I_v$ and $K_v$ are the modified Bessel functions of the first and second kinds of order $v$. The above equations can be rewritten in matrix form as

$$\begin{pmatrix} E_z^{(i)}(r) \\ -jH_z^{(i)}(r) \\ E_\theta^{(i)}(r) \\ -jH_\theta^{(i)}(r) \end{pmatrix} = M_i(r) \begin{pmatrix} C_i \\ D_i \\ C_i' \\ D_i' \end{pmatrix} \tag{5}$$

where $M_i(r)$ is the transfer matrix for the $i$th layer. According to electromagnetic boundary conditions, the azimuthal and longitudinal components of all fields must be continuous at layer boundaries, which results in

$$M_i(r_i) \begin{pmatrix} C_i \\ D_i \\ C_i' \\ D_i' \end{pmatrix} = M_{i+1}(r_i) \begin{pmatrix} C_{i+1} \\ D_{i+1} \\ C_{i+1}' \\ D_{i+1}' \end{pmatrix}, \qquad i = 1, 2, \cdots, m. \tag{6}$$

This way, the field coefficients in any layer can be expressed by those in its adjacent layer. In addition, due to the requirement that the field must be finite at both $r = 0$ and $r = \infty$, the coefficients in the first and last layers must satisfy $C_1' = D_1' = C_{m+1} = D_{m+1} = 0$, assuming that there are a total of $m + 1$ layers. Therefore, combining all the boundary conditions, fields in the first layer can be expressed by those in the last layer as

$$M_1(r_1) \begin{pmatrix} C_1 \\ D_1 \\ 0 \\ 0 \end{pmatrix} = M_2(r_1) M_2^{-1}(r_2) \cdots M_m(r_{m-1}) \times M_m^{-1}(r_m) M_{m+1}(r_m) \begin{pmatrix} 0 \\ 0 \\ C_{m+1}' \\ D_{m+1}' \end{pmatrix}. \tag{7}$$

This is a set of four equations containing four variables. For it to have a nontrivial solution, the determinant of the coefficient matrix must be zero, through which the propagation constant $\beta$ can be obtained. After solving for the propagation constant, the field components can be determined from the equations. An arbitrary constant will appear in the solution, which is determined by the total power carried by the mode. When compared to other methods, the advantage of this matrix formalism is that as the number of layers increases, it is only necessary to manipulate $4 \times 4$ matrixes, which is much more efficient than solving the large matrices that arise when solving for all the boundary conditions directly.

Once the field components are obtained, the transmission of the LPG can be calculated using coupled mode theory [14]. The refractive index profile of a grating structure can be expressed as

$$n(r, z) = n_0 \left\{ 1 + \sigma(z) \left[ 1 + m \cos\left( \frac{2\pi}{\Lambda} z \right) \right] \right\} \tag{8}$$

where $n_0$ is the original refractive index of the fiber core, $\sigma(z)$ is the slow varying envelope of the refractive index modulation, and $m$ is the index modulation strength of the grating. The coupling between different modes in a fiber can be described by the coupled mode equations

$$\frac{dA_\mu}{dz} = -j \sum_v A_\nu \left( K_{\nu\mu}^t + K_{\nu\mu}^z \right) \exp\left[ -j(\beta_\nu - \beta_\mu) z \right] + B_\nu \left( K_{\nu\mu}^t - K_{\nu\mu}^z \right) \exp\left[ j(\beta_\nu + \beta_\mu) z \right] \tag{9}$$

$$\frac{dB_\mu}{dz} = j \sum_v A_\nu \left( K_{\nu\mu}^t - K_{\nu\mu}^z \right) \exp\left[ -j(\beta_\nu + \beta_\mu) z \right] + B_\nu \left( K_{\nu\mu}^t + K_{\nu\mu}^z \right) \exp\left[ j(\beta_\nu - \beta_\mu) z \right] \tag{10}$$

where $A$ and $B$ are the amplitudes of the forward- and backward-propagating modes; $\mu$ and $\nu$ are the orders; and $\beta$ is the propagation constant of a certain mode. $K^t$ and $K^z$ are the transverse and longitudinal coupling coefficients defined by

$$K_{\nu\mu}^t = \omega \int\int \Delta\varepsilon \vec{E}_{t\nu} \cdot \vec{E}_{t\mu}^* r dr d\theta \tag{11}$$

$$K_{\nu\mu}^z = \omega \int\int \frac{\Delta\varepsilon \cdot \varepsilon}{\Delta\varepsilon + \varepsilon} \vec{E}_{z\nu} \cdot \vec{E}_{z\mu}^* r dr d\theta \tag{12}$$

where $\varepsilon$ and $\Delta\varepsilon$ are the permittivity and permittivity variations, respectively. By solving the above coupled mode equations, the transmission of LPG can be expressed as

$$T = \cos^2\left( \sqrt{\kappa^2 + \widehat{\sigma}^2} L \right) + \frac{\widehat{\sigma}^2}{\widehat{\sigma}^2 + \kappa^2} \sin^2\left( \sqrt{\kappa^2 + \widehat{\sigma}^2} L \right) \tag{13}$$

where

$$\kappa = \kappa_{1\nu-01}^{\text{cl-co}} = \kappa_{01-1\nu}^{\text{co-cl}^*} = \frac{m}{2}\tau$$

$$\widehat{\sigma} = \frac{\tau^{\text{co-co}}}{2} + \delta$$

and

$$\delta = \frac{1}{2} \left( \beta^{\text{co}} - \beta_\nu^{\text{cl}} - \frac{2\pi}{\Lambda} \right)$$

$$\tau_{\nu\mu}(z) = \frac{\omega \varepsilon_0 n_0^2 \sigma}{2} \int_0^{2\pi} d\theta \int_0^\infty r dr \vec{E}_{t\nu} \cdot \vec{E}_{t\mu}^*.$$

From (13), much of the useful information of the LPG can be determined, including the on-resonance transmission

$$T = \cos^2(\kappa L) \tag{14}$$

the resonant wavelength

$$\lambda_0 = \frac{n_{\text{eff}}^{\text{co}} - n_{\text{eff}}^{\text{cl}}}{1 - \tau^{\text{co-co}} \frac{\Lambda}{2\pi}} \Lambda \tag{15}$$

and the relative bandwidth for weak gratings

$$\frac{\Delta\lambda}{\lambda} = \frac{2}{N}. \tag{16}$$

This theoretical model is applicable to both all-dielectric LPG structures and an LPG containing metallic layers. To include

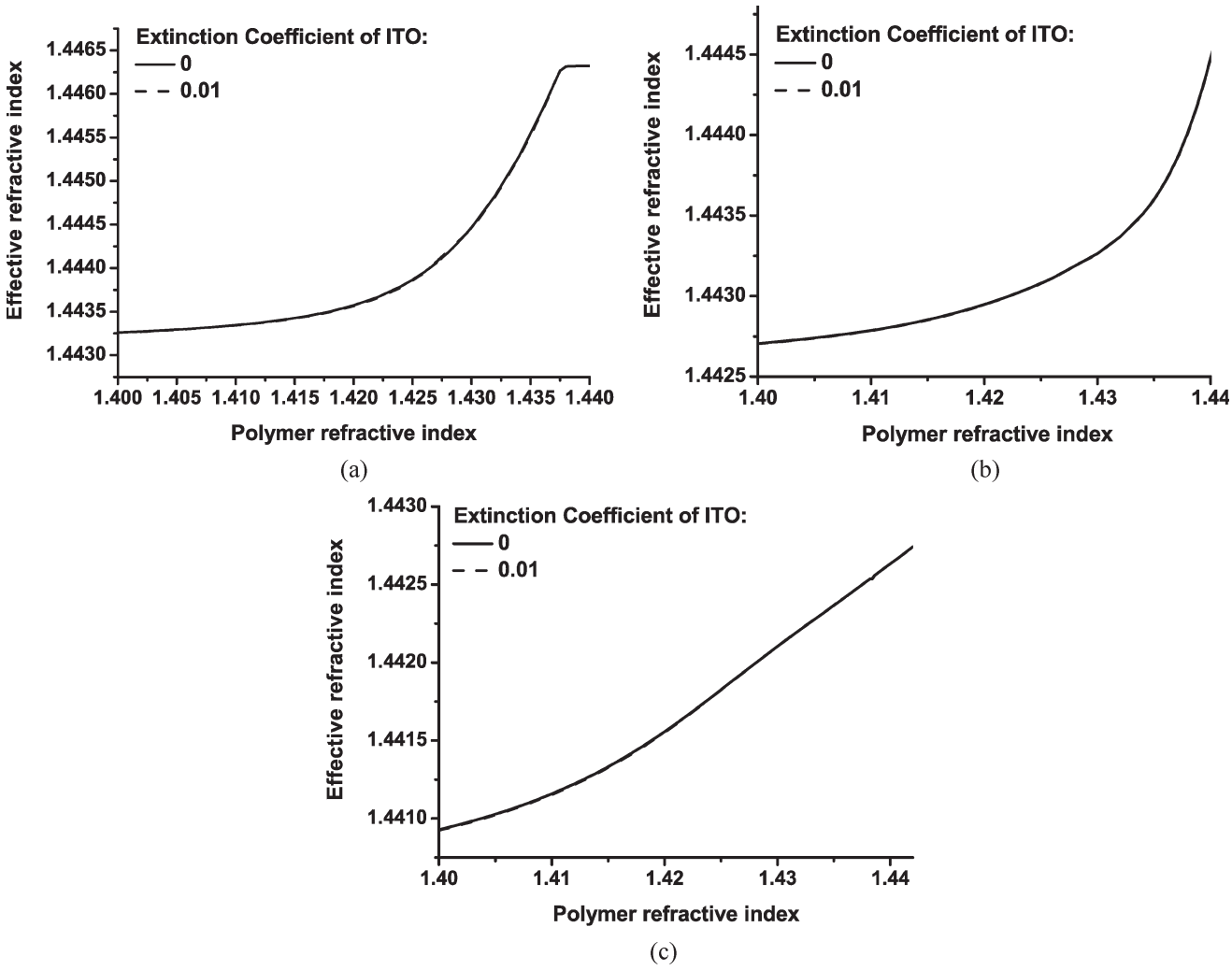


Fig. 2. Calculated real portion of the effective refractive indices of the first silica cladding layer as a function of the refractive indices of E-O polymer layer under the conditions with and without the absorption of ITO layer. Other ITO layer parameters are $n = 1.8$ and thickness $t = 50$ nm. (a) First cladding mode. (b) Second cladding mode. (c) Third cladding mode.

metallic layers, it is only necessary to change the real refractive indices for dielectric materials into the complex refractive index of metals.

Based on the above theoretical model, we have quantitatively analyzed the tuning characteristics of the LPG filter by considering the first four layers [i.e., layers 1–4, as shown in Fig. 1(b)]. First, it is important to check the difference between treating ITO as a pure dielectric layer and as an absorbing layer. The ITO material parameters we are using are based on the data from [18]. The condition used in our sputtering is 5 mtorr (or 0.67 Pa) at room temperature without additional oxygen gas. Under this condition, we use Sellmeier's equation to find that the refractive index of ITO at 1550 nm is around 1.8. Also, according to the data in the literature [18], the optical extinction coefficient of the ITO in our condition should be lower than 0.01. To check whether the absorption of the ITO plays a key role in the tuning characteristics, we calculate both the real and the imaginary portions of the effective refractive index of the thin silica cladding layer $n_{\text{eff}}^{\text{cl}-i}$ for different cladding modes with an ITO extinction constant of $k = 0$ (corresponding to the case of no absorption) and $k = 0.01$ (corresponding to the case of maximum absorption), respectively. We further assume that the refractive index and the thickness of the ITO layer are $n = 1.8$ and 50 nm, respectively. Fig. 2(a)–(c) shows the calculated real portions of the effective refractive indices of the first, second, and third cladding modes of the silica cladding layer, respectively, as a function of the refractive index of polymer layer [i.e., layer 4, as shown in Fig. 1(b)]. Similarly, Fig. 3(a)–(c) shows the calculated imaginary portions of the effective refractive indices (i.e., corresponding to the attenuation constants) of the first-, second-, and third-order cladding modes of the thin silica cladding layer, respectively, as a function of polymer layer. These two figures clearly suggest that 1) the influence of the absorption of the ITO layer on the real portion of the effective refractive index of the silica cladding layer is negligible; 2) sensitivity of the effective refractive indices of the first and second modes increases as the refractive index of the polymer layer increases; 3) attenuation constants are really small, which allows us to ignore their influence in the future calculation; and 4) the ITO layer can be treated as a high refractive index overlay because its refractive index is higher than that of silica.

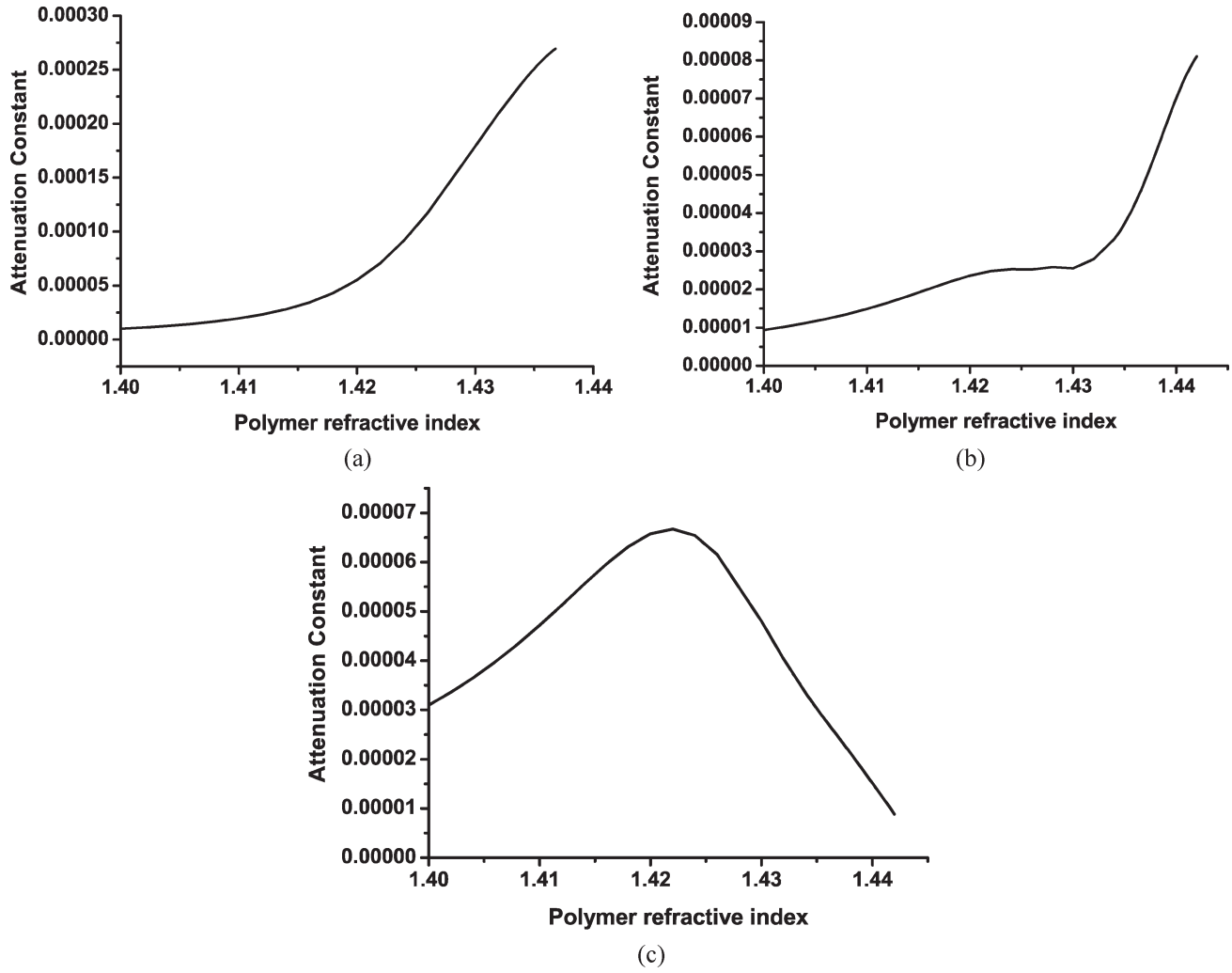


Fig. 3. Calculated imaginary portion of the effective refractive indices of the first silica cladding layer as a function of the refractive indices of the E-O polymer layer under the conditions with and without the absorption of ITO layer. Other ITO layer parameters are $n = 1.8$ and thickness $t = 50$ nm. (a) First cladding mode. (b) Second cladding mode. (c) Third cladding mode.

To quantitatively investigate the tuning enhancement effect due to the existence of this high refractive index overlay, we calculate the transversal mode field distributions for the first three lowest order modes with and without the ITO overlay. Figs. 4–6 depict the calculated transversal mode distributions for cladding modes 1, 2, and 3, respectively. These calculation results verify that indeed, there are substantial changes in mode field distributions due to the existence of the ITO overlay. The higher refractive index of the ITO overlay causes more light energy to concentrate near the outside polymer layer, which results in an increased tuning range. This tuning enhancement effect is further confirmed by analyzing the effective refractive indices of the modes in the thin silica cladding layer as a function of the refractive index of the polymer for cases with and without the ITO overlay. Fig. 7(a)–(c) illustrates the calculated refractive indices of cladding modes 1, 2, and 3, respectively, as a function of the outside polymer layer refractive index for the cases with and without the ITO overlay. It can clearly be seen that the up-slopes are significantly steeper (in particular, more than ten times increase in slope for cladding mode 1 when the polymer refractive index is tuned from 1.425 to 1.435) due to the existence of ITO overlay.

## III. Experimental Results

### A. E-O Polymer Synthesis

To experimentally confirm the tuning enhancement effect as suggested by the four-layer theoretical model, we first synthesized poly(vinylidene fluoride-trifluoroethylene-chlorofluoroethylene) (PVDF-TrFE-CFE) terpolymer. The repeat unit of PVDF, $CH_2CF_2$ carries a vacuum dipole moment of about $7 \times 10^{-30}$ Cm associated with the positive hydrogen and negative fluorine atoms. Because such dipoles are rigidly attached to main-chain carbons, their orientation is directly controlled by the conformation and packing of molecules. An all-*trans* conformation induces the alignment of the $CH_2CF_2$ dipoles in the zigzag plane and perpendicular to the chain axis. Due to the existence of this dipole structure (i.e., the dipoles are connected together), it is difficult to switch the polarization direction of the dipoles. By introducing a random termonomer, chlorofluoroethylene (CFE), into P(VDF-TrFE) to form terpolymer P(VDF-TrFE-CFE), the crystalline structure of P(VDF-TrFE) can be substantially weakened by reducing the size of the coherent polarization regions to a nanometer scale through the introduction of defects [9]. It has been found that

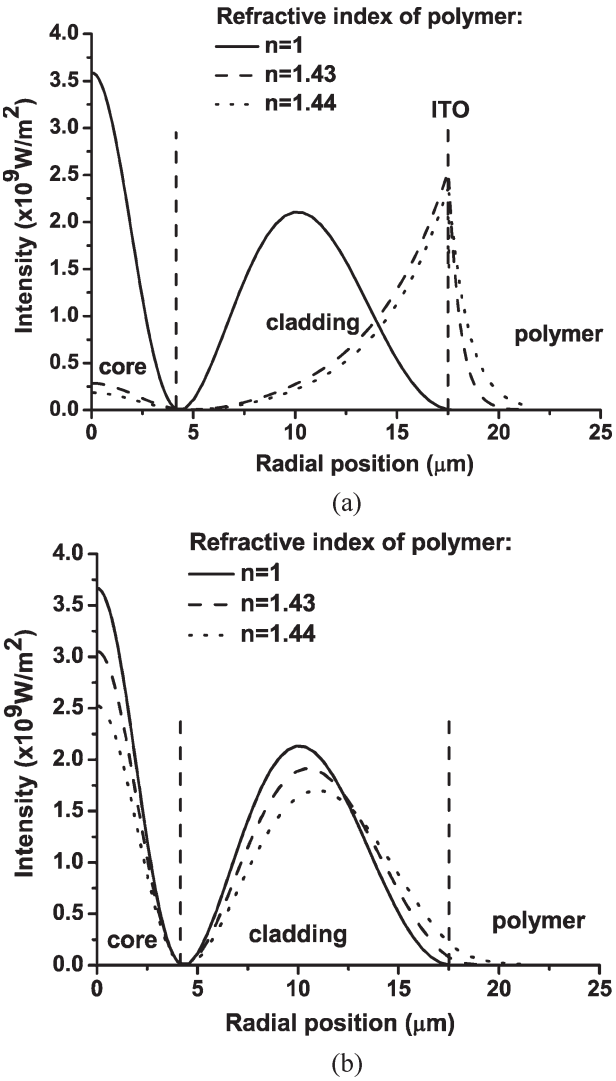


Fig. 4. Transversal electric field distributions of silica cladding modes under the cases with and without ITO overlay for the first cladding mode. (a) With ITO. (b) Without ITO.

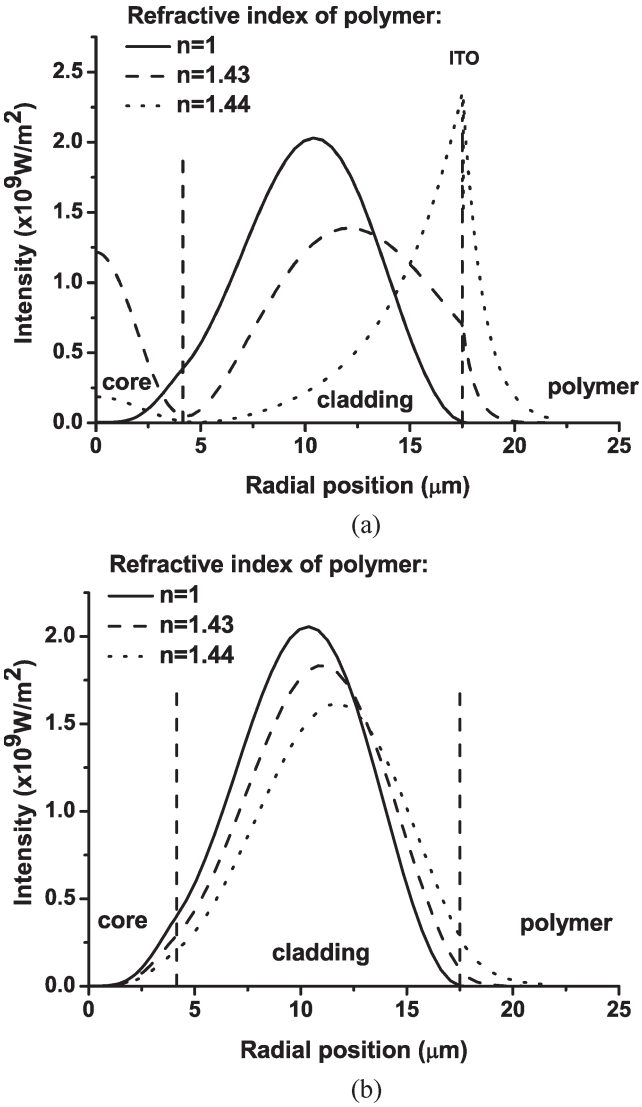


Fig. 5. Transversal electric field distributions of silica cladding modes under the cases with and without ITO overlay for the second cladding mode. (a) With ITO. (b) Without ITO.

under a proper ratio among the three monomers in the terpolymer, a Kerr effect induced relative refractive index change of $-2.6\%$ can be achieved in a freestanding film under an electric field of 80 MV/m, and 0.52% change can be achieved in a film on a substrate under an electric field of 100 MV/m [10]. The E-O effects in freestanding film and substrate-clamped film generate refractive index changes in the opposite direction. As a result, if the terpolymer film is partially clamped, the canceling between these two effects may reduce the overall refractive index change. Therefore, the terpolymer is completely clamped by embedding it in epoxy when it is used for the E-O tunable LPG filter application. The refractive index of the terpolymer is measured by an ellipsometer and is around 1.41 at 633 nm, which is slightly lower than that of the fiber cladding ($n_{\mathrm{clad}} = 1.4441$ at 1550 nm).

However, as shown in Fig. 7, the filter has an optimized tuning range when the refractive index of the outside polymer layer is around 1.43, which is close to the refractive index of the silica layer. To tune the refractive index of the polymer layer to the optimized refractive index region, we developed a new nanocomposite E-O terpolymer. Zinc sulfide (ZnS) nanoparticles were dispersed in the terpolymer matrix. Because ZnS has a refractive index of around 2.27 at 1550 nm, the dispersion of ZnS nanoparticles can increase the overall refractive index of the polymer layer. To ensure that the ZnS nanoparticles were uniformly dispersed, the chemically functionalizing approach was harnessed for nanoparticle dispersion. It was found that by adding around 10% concentration of ZnS nanoparticle, the overall refractive index of the polymer layer was increased to the optimized level of 1.43. Fig. 8 illustrates the structure of ZnS nanoparticle-dispersed E-O terpolymer.

### *B. Experimental Results of Tuning Range Enhancement*

The fibers used in the experiments were Newport F-SBG-15 photosensitive single-mode fibers, which have refractive indices of $n_{\mathrm{core}} = 1.4491$ and $n_{\mathrm{clad}} = 1.4441$, and diameters of $d_{\mathrm{core}} = 8.3$ $\mu$m and $d_{\mathrm{clad}} = 125$ $\mu$m, respectively. Before

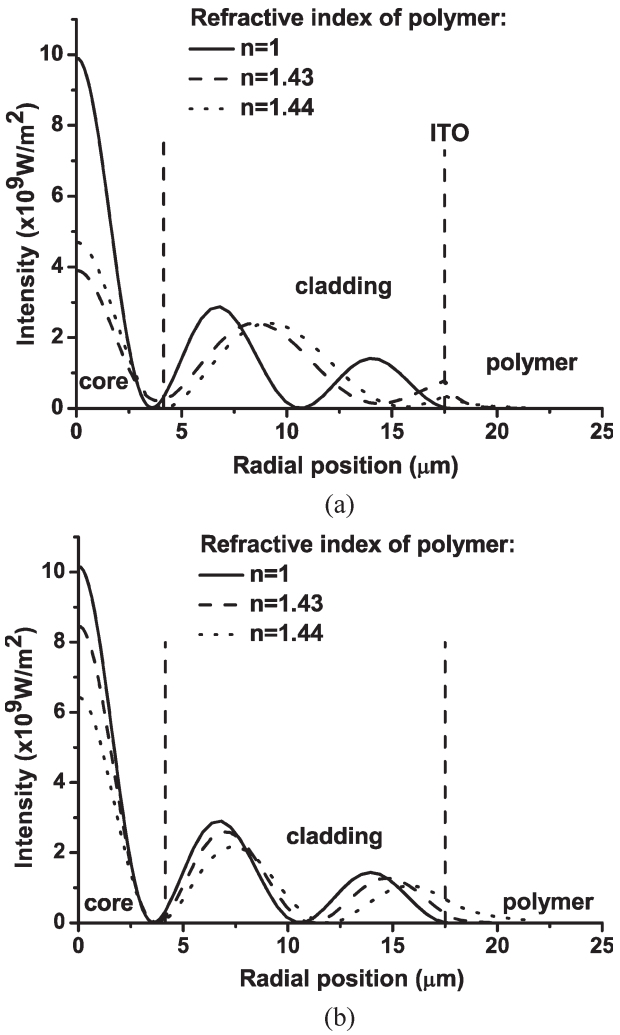


Fig. 6. Transversal electric field distributions of silica cladding modes under the cases with and without ITO overlay for the third cladding mode. (a) With ITO. (b) Without ITO.

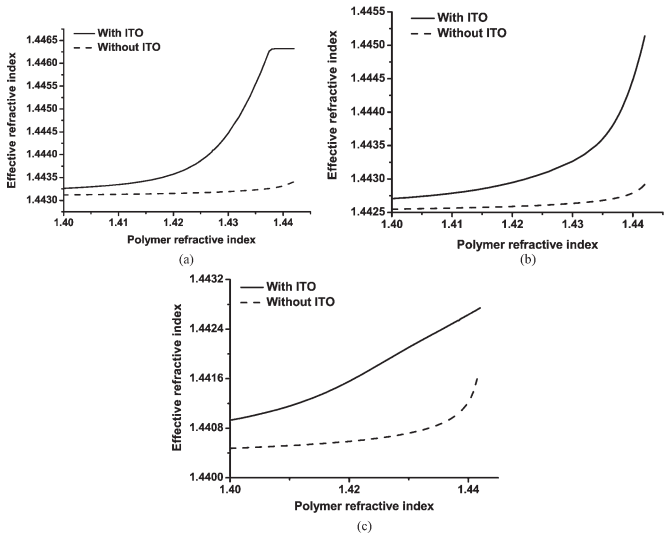


Fig. 7. Effective refractive index of different silica layer cladding modes as a function of polymer layer under the cases with and without ITO overlay. Other calculation parameters are ITO refractive index: 1.8; ITO thickness: 50 nm and wavelength: 1500 nm.

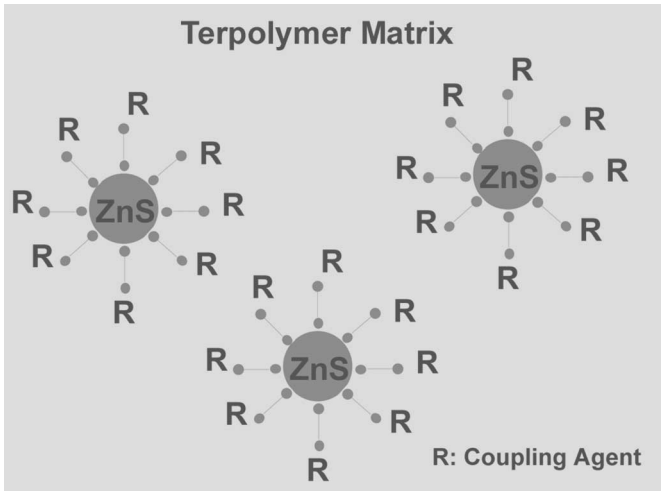


Fig. 8. Configuration of ZnS nanoparticle–terpolymer composition.

writing gratings, the jacket of the fiber was stripped off, and the diameter of the fiber was reduced to around 40 $\mu$m through hydrofluoric acid etching. Reducing the cladding thickness provides a single resonant band in the LPG spectrum and an enhancement in the tuning sensitivity [6], [7]. The grating was written by passing UV-irradiation from a frequency-doubled argon laser through an amplitude mask. After grating fabrication, the ITO electrode was deposited on fiber by sputtering. The terpolymer was deposited on the ITO-coated fiber by a modified dip-coating process. The terpolymer was first dissolved in methyl ethyl ketone (MEK), and a suitable viscosity of solution was achieved by concentrating. The solution was then poured into a die with a large orifice on the top and a small orifice at the bottom. When the fiber was drawn downward through the die, a thin uniform layer of solution formed on the surface of the ITO-coated fiber, and after the quick evaporation of MEK, a cylindrical thin film of polymer was deposited on the fiber. The thickness of the polymer layer can be adjusted by both the solution concentration and the drawing rate. Once the polymer layer had been applied, a thin layer of gold was sputtered on top of the polymer layer to serve as the outer electrode. Furthermore, a small section of polymer was washed away with acetone to open a contact window for the inner ITO electrode and a conducting adhesive was used to wire out the electrodes. Finally, the terpolymer was completely clamped by applying epoxy to the LPG.

To experimentally check the tuning range enhancement effect, we measured the LPG tuning range for the same amount of layer 4 refractive index (i.e., corresponding to the polymer layer) variations under the cases with and without ITO overlay. An index matching oil was used to provide the required refractive index variation. Fig. 9(a) and (b) illustrates the LPG spectra as a function of the refractive index of layer 4 for the cases with and without the ITO overlay. These experimental results show that a general trend for both kinds of LPGs (i.e., with and without the ITO layer) was that as the external (layer 4) index increased, the resonant wavelength $\lambda_0$ gradually shifted to shorter wavelength, while the depth and shape of the

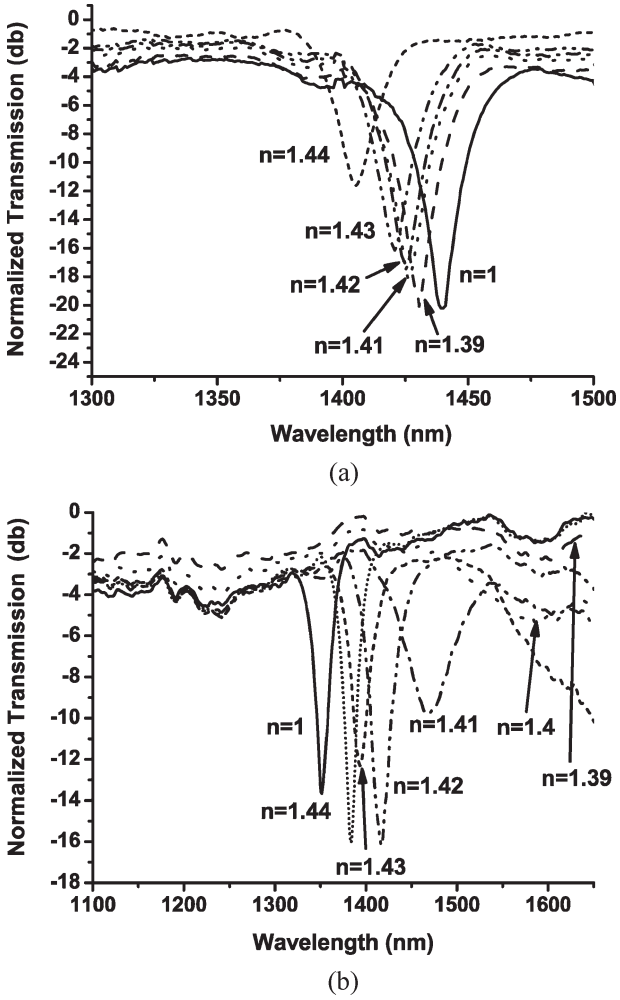


Fig. 9. Experimentally measured spectra of the LPG as a function of outsider refractive index under the cases. (a) Without ITO overlay. (b) With ITO overlay.

attenuation peak also underwent some changes. However, for the LPG without the ITO overlay, the peak always remained on the shorter wavelength side of the original peak (i.e., the peak position in ambient air, $n = 1$) as $n$ changed from 1 to 1.44. On the other hand, for the LPG with the ITO overlay, as the external refractive index increased, the peak disappeared quickly and came back again from the longer wavelength side. Furthermore, tuning sensitivity was significantly enhanced. For instance, as the refractive index of the outside layer changed from 1.41 to 1.42, the corresponding spectrum shifts were 5 nm for the LPG without ITO and 53 nm for the LPG with ITO, respectively. The ITO overlay caused a more than tenfold increase in tuning range.

This enhanced tuning range was also experimentally demonstrated by electrically tuning the LPG. An electrically tunable LPG filter sample was fabricated using the procedures described at the beginning of this section. By applying an electric field of 50 $\mathrm{V}/\mu$m, a tuning range as large as 50 nm was achieved, as shown in Fig. 10. We also measured the refractive index change of the polymer under the same level of electric field; it was found that the refractive index change was around $1\%$. This tuning range is consistent with the theoretical analysis

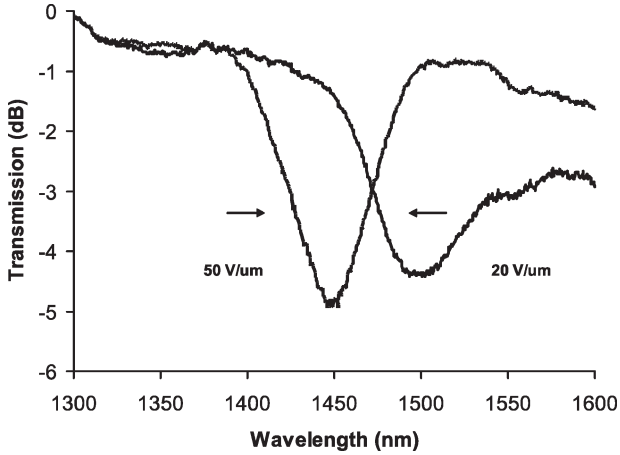


Fig. 10. Tuning spectra of the LPG under different magnitudes of applied electric field.

result, as depicted in Fig. 9. Therefore, a significantly enhanced tuning range was realized by the ITO overlay.

## IV. Conclusion

In conclusion, we have quantitatively analyzed the electrically tunable LPG filter using a precision four-layer model. It showed that the tuning range of the filter could be significantly enhanced (ten plus fold) due to the existence of the high refractive index ITO layer. The experimental results agreed well with the theoretical predictions. A tuning range as large as 50 nm was achieved when applying an electric field of 50 $\mathrm{V}/\mu$m on the E-O polymer. Furthermore, the refractive index of the P(VDF-TrFE-CFE) terpolymer was optimized by dispersing ZnS nanoparticles into the polymer matrix so that the maximum tuning range could be achieved with the same amount of refractive index variation. This unique all-fiber electronically tunable filter has the advantages of low insertion loss, large tuning speed, low power consumption, and high reliability because there are no moving parts. The potential applications of this electrically tunable LPG include high-speed reconfigurable communication systems, ultrasensitive fiber optic sensors, and low cost, compact size, and high-speed spectrometers.

## References

[1] N. Grote and H. Venghaus, *Fiber Optic Communication Devices*. Berlin, Germany: Springer-Verlag, 2001, ch. 7.

[2] A. M. Vengsarkar, P. J. Lemaire, J. B. Judkins, V. Bhatia, T. Erdogan, and J. E. Sipe, "Long-period fiber gratings as band-rejection filters," *J. Lightw. Technol.*, vol. 13, no. 1, pp. 58–65, Jan. 1996.

[3] F. Cattaneo, K. Baldwin, S. Yang, T. Krupenkine, S. Ramachandran, and J. A. Rogers, "Digitally tunable microfluidic optical fiber devices," *J. Microelectromech. Syst.*, vol. 12, no. 6, pp. 907–912, Dec. 2003.

[4] A. A. Abramov, B. J. Eggleton, J. A. Rogers, R. P. Espindola, A. Hale, R. S. Windeler, and T. A. Strasser, "Electrically tunable efficient broadband fiber filter," *IEEE Photon. Technol. Lett.*, vol. 11, no. 4, pp. 445–447, Apr. 1999.

[5] X. Dong, X. Yang, P. Shum, and C. C. Chan, "Tunable WDM filter with 0.8-nm channel spacing using a pair of long-period fiber gratings," *IEEE Photon. Technol. Lett.*, vol. 17, no. 4, pp. 795–797, Apr. 2005.

[6] S. Yin, Q. Zhang, K. W. Chung, R. Yang, Z. Cheng, and Y. Lu, "Investigation of the electro-optic properties of electron-irradiated poly(vinylidene fluoride-trifluoroethylene) copolymer," *Opt. Eng.*, vol. 39, no. 3, pp. 670–672, Mar. 2000.

[7] K. W. Chung and S. Yin, "Analysis of a widely tunable long-period grating by use of an ultrathin cladding layer and higher-order cladding mode coupling," *Opt. Lett.*, vol. 29, no. 8, p. 812, Apr. 2004.
[8] Q. M. Zhang, V. Bharti, and X. Zhao, "Giant electrostriction and relaxor ferroelectric behavior in electron-irradiated poly(vinylidene fluoride-trifluorotehylene) copolymer," *Science*, vol. 280, no. 5372, pp. 2101–2104, Jun. 1998.
[9] F. Xia, Z. Y. Cheng, H. Xu, Q. M. Zhang, G. Kavarnos, R. Ting, G. Abdul-Sedat, and K. D. Belfield, "High electromechanical responses in terpolymer of poly(vinylidene fluoride-trifluoroethylene-chlorofluoroethylene)," *Adv. Mater.*, vol. 14, no. 21, pp. 1574–1577, Nov. 2002.
[10] D. Y. Jeong, Y. K. Wang, M. Huang, Q. M. Zhang, G. J. Kavarnos, and F. Bauer, "Electro-optical response of the ferroelectric relaxor poly(vinylidene fluoride-trifluoroethylene-chlorofluoroethylene) terpolymer," *J. Appl. Phys.*, vol. 96, no. 1, pp. 316–319, Jul. 2004.
[11] I. D. Villar, I. R. Matias, F. J. Arregui, and P. Lalanne, "Optimization of sensitivity in long period fiber gratings with overlay deposition," *Opt. Express*, vol. 13, no. 1, pp. 56–69, Jan. 2005.
[12] Z. Wang, J. R. Heflin, R. H. Stolen, and S. Ramachandran, "Analysis of optical response of long period fiber gratings to nm-thick thin-film coatings," *Opt. Express*, vol. 13, no. 8, pp. 2808–2813, Apr. 2005.
[13] A. Cusano, A. Iadicicco, P. Pilla, L. Contessa, S. Campopiano, and A. Cutolo, "Mode transition in high refractive index coated long period gratings," *Opt. Express*, vol. 14, no. 1, pp. 19–34, Jan. 2006.
[14] T. Erdogan, "Cladding-mode resonances in short- and long-period fiber grating filters," *J. Opt. Soc. Amer. A, Opt. Image Sci.*, vol. 14, no. 8, pp. 1760–1773, Aug. 1997.
[15] E. Anemogiannis, E. N. Glytsis, and T. K. Gaylord, "Transmission characteristics of long-period fiber gratings having arbitrary azimuthal/radial refractive index variation," *J. Lightw. Technol.*, vol. 21, no. 1, pp. 218–227, Jan. 2003.
[16] C. Yeh and G. Lindgren, "Computing the propagation characteristics of radially stratified fibers: An efficient method," *Appl. Opt.*, vol. 16, no. 2, pp. 483–493, Feb. 1977.
[17] M. J. Adams, *An Introduction to Optical Waveguides*. New York: Wiley, 1981.
[18] Y. S. Jung, "Spectroscopic ellipsometry studies on the optical constants of indium tin oxide films deposited under various sputtering conditions," *Thin Solid Films*, vol. 467, no. 1/2, pp. 36–42, Nov. 2004.

**Qin Chen** was born in Jiangxi, China, on May 28, 1983. He received the B.S. degree in electronic science and technology with the major in optoelectronics from Tsinghua University, Beijing, China, in June 2003. He is currently working toward the Ph.D. degree at the Department of Electrical Engineering, Pennsylvania State University, University Park.

His research interests include polymeric electrooptic materials and the development of advanced photonic devices such as fiber gratings, photonic crystals, and surface plasmon-based devices.

**Jonathan Lee** received the B.S. degree in electrical engineering from Princeton University, Princeton, NJ, in 2002 and the M.S. degree in electrical engineering from the Pennsylvania State University, University Park, in 2005. He is currently working toward the Ph.D. degree at the Department of Electrical Engineering, Pennsylvania State University.

He has a solid background in the development and the production of advanced photonic devices. In particular, he is very familiar with fiber optic devices and clean room fabrication processes. He has also been the author or coauthor of several journal papers and conference proceedings.

**Minren Lin**, photograph and biography not available at the time of publication.

**Yong Wang** was born in Jiangsu, China, on August 12, 1978. He received the B.S. and M.S. degrees in physics from Nanjing University, Nanjing, China, in 1999 and 2002, respectively. He is currently working toward the Ph.D. degree with the Department of Electrical Engineering, Pennsylvania State University, University Park.

**Stuart (Shizhuo) Yin** (M'95–SM'97) received the Ph.D. degree in electrical engineering from the Pennsylvania State University, University Park, in 1993.

He has over 20 years of experience in the research and development of advanced photonic devices. He has successfully managed many research projects supported by a variety of U.S. government agencies, including the Defense Advanced Research Projects Agency (DARPA), the National Science Foundation, the National Institute of Standards and Technology, the Army Research Office, the U.S. Army Missile Command, and the U.S. Navy. He is an Associate Professor with the Department of Electrical Engineering, Pennsylvania State University. He holds two U.S. patents: one for a magneto-optic switching and the other for a fast-speed tunable fiber optic filter. He has also authored or coauthored 12 books, over 90 referred journal papers, and over 100 conference proceedings.

Dr. Yin was a Fellow of the International Society for Optical Engineering (SPIE) and a member of the Optical Society of America. Since 1996, he has served as the Co-Chair of SPIE conferences on photorefractive fiber and crystal devices. He also serves on the reviewing panels of the National Institute of Standards and Technology and the National Science Foundation. He is also the Associate Editor of the *International Journal of Optical Neural Networks*. He was the recipient of the 1996 U.S. Army Young Investigator Award.

**Qiming Zhang** (M'97–SM'99) received the Ph.D. degree in solid state physics from the Pennsylvania State University, University Park, in 1986.

He is a Professor of electrical engineering at Pennsylvania State University. He has been working on polar and multifunctional materials and devices, especially polymeric-based materials and devices, for many years and has made several important contributions to this field. He has authored and coauthored over 250 publications and delivered many invited talks in these areas. His group discovered and developed the ferroelectric relaxor polymer, which is the first relaxor reported in polymers and possesses a room temperature dielectric constant higher than 50, an electrostrictive strain higher than 7%, and an electric energy density near 10 J/cm$^3$. His group has also developed nanocomposites based on delocalized electron organic systems, resulting in very high dielectric constant ($\sim$ 1000), which can generate high induced strain with the elastic energy density $>$ 1 J/cm$^3$ under a relatively low field of $\sim$ 23 MV/m. More recently, his group has explored the concept of reversible polar-to-nonpolar transformation in polymers and interface effects in nanocomposites to achieve high electric energy density for pulse power capacitors.

**Karl M. Reichard** (S'84–M'85), photograph and biography not available at the time of publication.